Optics & Laser Technology 167 (2023) 109839

Contents lists available at ScienceDirect

Optics and Laser Technology

journal homepage: www.elsevier.com/locate/optlastec

Full length article

InP-based quantum dot on-chip white LEDs with optimal circadian efficiency

Jeroen Cerpentier [a,*], Bega Karadza [a], Hannes van Avermaet [b,c], Luca Giordano [b,c], Pieter Schiettecatte [b,c], Zeger Hens [b,c], Youri Meuret [a]

[a] KU Leuven, Department of Electrical Engineering (ESAT), Light & Lighting Laboratory, B-9000 Gent, Belgium
[b] Physics and Chemistry of Nanostructures, Department of Chemistry, Ghent University, B-9000 Gent, Belgium
[c] Center for Nano and Biophotonics, Ghent University, B-9000 Gent, Belgium

ARTICLE INFO

Keywords:
Solid-state lighting
LED
Quantum dot
Circadian effect

ABSTRACT

Solid-state light-emitting diodes (LEDs) are capable of reaching high visual performance, both in terms of efficiency and color quality. The lighting industry is however increasingly considering the non-visual, biological effects of light. These non-visual or circadian effects can be quantified by considering the overlap of the light source spectrum with the melanopic action spectrum. To ensure optimal visual and non-visual impact of LED-based light sources, high spectral flexibility is required. This can be achieved with multi-channel systems and specific color-converting materials such as quantum dots (QDs). Despite their flexibility, multi-channel systems come with increasing system complexity and cost. This paper presents a simulation-based design method for single-chip InP-based QD on-chip white LEDs that achieve state-of-the art circadian performance while maintaining visual performance. These results are experimentally replicated by fabricating single-chip QD-LEDs with 3 types of InP-based QDs (including cyan-emitting) that set a new standard for spectral circadian performance.

1. Introduction

Solid-state light sources, in particular light-emitting diodes (LEDs), have dominated the commercial lighting scene over the past decades, due to their benefits in terms of efficiency, lifetime and compactness [1]. Evaluation of LED performance is typically done by considering the luminous efficacy (LE, lm W^{-1}), i.e. the visual light produced versus the electrical power consumed, and the color rendering index (CRI R_a). If a modern lighting system performs poorly on both metrics, it is generally not applicable for commercialization [2,3]. The CRI R_a is gradually being replaced by the more complete TM-30 color fidelity R_f, which considers color rendering of 99 samples instead of 8 [4,5]. But light also has important non-visual consequences. Over the last decades, physiologists have studied the biological effects of light, and found that light significantly impacts the circadian rhythm [6,7]. Light influences the human biological clock via the intrinsically photosensitive retinal ganglion cells (ipRGCs), located at the eye retina. These ipRGCs excrete melanopsin, which is strongly linked with the production of the sleep hormone melatonin [8,9]. Importantly, the production of melanopsin by the ipRGCs depends on the wavelength of the incident light on these photoreceptors. This wavelength dependency is officially described by the CIE-defined melanopic action spectrum $C(\lambda)$ (CIE S026/E:2018), which is the circadian equivalent of the photopic luminous efficiency function $V(\lambda)$ (Fig. 1a), and allows quantitative assessment of the melanopic impact of a certain spectral power distribution (SPD). Since melanopsin production has a significant impact on melatonin, it is commonly regarded as a proxy to determine the circadian effects of light [10]. Having such measures for the biological impact of light allows lighting designers to consider these non-visual effects. This is done within the field of human centric lighting (HCL), in which both the visual and biological response of humans to light is taken into account [11].

Following the discovery of melanopsin, various HCL systems have been designed. Since both visual and non-visual effects are considered, high spectral flexibility is required, especially when taking into account that energy efficiency and color rendering cannot be neglected. Spectral engineering of white LEDs is mainly done by using wavelength-conversion materials, typically phosphors [12,13]. This is directly linked to the fact that the efficacy of multi-chromatic LEDs is hampered by the green gap of LED technology [14]. In order to achieve specific LED emission spectra, quantum dots (QDs) have seen increasing interest over the last years [15–17]. This can mainly be attributed to their narrow emission spectrum and flexible peak wavelength, which depends on the size of these nanoparticles [18,19]. By combining multiple narrow-band QD-LEDs in a multi-channel configuration, high

* Corresponding author.
E-mail address: jeroen.cerpentier@kuleuven.be (J. Cerpentier).

https://doi.org/10.1016/j.optlastec.2023.109839
Received 3 April 2023; Received in revised form 13 June 2023; Accepted 13 July 2023
Available online 24 July 2023

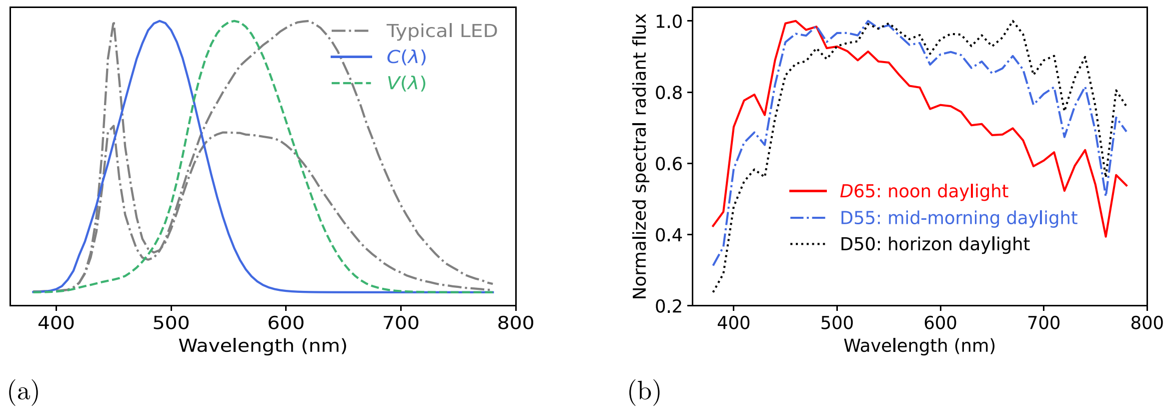

Fig. 1. **(a)** Comparison of the melanopic action spectrum $C(\lambda)$ with the photopic efficiency curve $V(\lambda)$. For two typical white LED spectra, it is clear that there is a strong overlap with $V(\lambda)$, whereas the overlap with $C(\lambda)$ is limited. **(b)** Comparison of the normalized spectral power distribution of D_{65}, D_{55} and D_{50} daylight illuminants.

spectral flexibility can be achieved [3,20,21]. Although such multi-channel systems perform well both in terms of visual and non-visual effects, they have some important disadvantages. First of all, a complex driving circuitry, as well as multiple QD-based LEDs are required. Sufficient color mixing of the emission spectra of the individual LEDs is challenging, often resulting in a significant decrease in efficiency. Furthermore, ensuring stable color emission typically requires advanced control systems [22,23]. This results in more expensive light sources compared to white, single-chip LEDs. In addition, various of these systems use cadmium-based QDs, which is a restricted element in many countries, under the RoHS and similar directives [15].

In this paper, single-chip QD-LEDs with high circadian performance are investigated and demonstrated. The used QDs are InP-based, which are increasingly considered for QD-LEDs, due to their large absorption cross section, broad wavelength coverage and narrow emission spectrum [24]. Moreover, InP-based QDs pose less toxicity issues compared to Cd/Pb alternatives [25]. It has recently been shown that InP-based QDs even have the potential to reach near-unity photoluminescence quantum yield across the entire visible spectrum [26,27]. These merits make InP-based QDs highly suitable for the spectral flexibility imposed by HCL. Red-emitting InP-based QDs have already been combined with traditional green/yellow powder phosphors in order to obtain efficient white LEDs with high color rendering [15], but for the high spectral constraints that are imposed on HCL LEDs, the emission spectrum of these phosphors is likely too wide. Alternatively, this study considers a single blue LED chip combined with multiple, on-chip InP-based QDs. This configuration is similar to an RGB QD-LED configuration, which has only recently been demonstrated with high efficacy, due to the important problem of QD re-absorption losses [28,29].

The paper starts off by providing a brief summary of the relevant circadian metrics and the state-of-the-art, followed by an optimization procedure that relies on a representative optical simulation model of an on-chip color-conversion mixture with 3 types of QDs, in order to reach optimal circadian performance. One of the most promising results is then experimentally replicated by mixing the required InP-based quantum dot particles into a thiol-ene resin, which is UV-cured onto a blue LED chip. The results show that, while maintaining color rendering and whiteness, record-breaking circadian performance is obtained by integrating cyan-emitting InP-based QDs in the QD-LED configuration. This result is followed by a discussion on the trade-off between circadian performance and energy efficiency, as well as how to deal with QD re-absorption losses, which are highly present in this case due to the usage of cyan-emitting QDs at high concentration. To end, we take this important trade-off into account to design and demonstrate a more energy efficient circadian QD-LED, which includes an extraction dome with cyan-emitting QDs in order to reduce re-absorption effects. This final QD-LED provides state-of-the art performance in terms of circadian luminous efficacy of radiation, while only using a single LED chip.

2. Background

Having a spectral power distribution of light $S(\lambda)$ in W nm^{-1}, the melanopic action spectrum $C(\lambda)$ allows for calculation of the emitted *circadian power* – the melanopic radiant flux – defined over the human visible spectrum as [30]:

$$\Phi_{mel} = \int_{380}^{780} S(\lambda)C(\lambda)d\lambda. \tag{1}$$

This quantity is useful as a measure for melanopic effects, but metrics including the luminous flux are more frequently used. In 2018, the CIE introduced the melanopic efficacy of luminous radiation (MELR) as the ratio between the melanopic radiant flux and luminous flux:

$$K_{mel,v} = \frac{1000 \times \Phi_{mel}}{683.002 \times \int_{380}^{780} S(\lambda)V(\lambda)d\lambda}. \tag{2}$$

This results in a quantity in mW/lm, intuitively representing the amount of melanopic power per visual response. Due to the relevance of natural daylight within our daily lives, it is an important reference to compare with. There are different standard illuminants that are used to represent the spectrum of daylight (Fig. 1b), of which D_{65} is the most common. Given the spectral power distribution D_{65}, a new dimensionless quantity can be considered that scales the light source's MELR relevant to that of D_{65}; the CIE-defined melanopic daylight efficacy ratio (MDER) [30,31]:

$$\mathrm{MDER} = \frac{K_{mel,v}}{K_{mel,v}^{D_{65}}} = \frac{K_{mel,v}}{1.326}, \tag{3}$$

A value larger than 1 for MDER consequently implies that the light source has a higher MELR than the D_{65} illuminant.

In human centric lighting, it is important that the SPD of a white light source corresponds with the environmental setting, e.g. low MDER at night and higher MDER during the morning or in an office environment. Most white LEDs have fairly low MDER values (≤0.75) for different correlated color temperatures (CCTs), as indicated by Schlangen et al. (2021) [30]. This is due to the fact that white LEDs are typically designed to have high luminous efficacy without considering the circadian effects (Fig. 1a). In a previous publication, we studied the theoretical spectral MDER boundaries under different color rendering, D_{uv} and CCT constraints [32]. These theoretical limits are shown in Fig. 2 for $R_f \geq 80$, together with the MDER values for the reference D_{50}, D_{55} and D_{65} illuminants. When including the MDER values of some typical white LEDs within these boundaries, it is clear that relatively low MDER is obtained for all CCTs. In order to expand this MDER range, several companies have developed white LEDs that target high MDER. The MDER values of these LEDs are also shown in Fig. 2 and they demonstrate clearly higher MDER, but still leave ample room for further improvement.

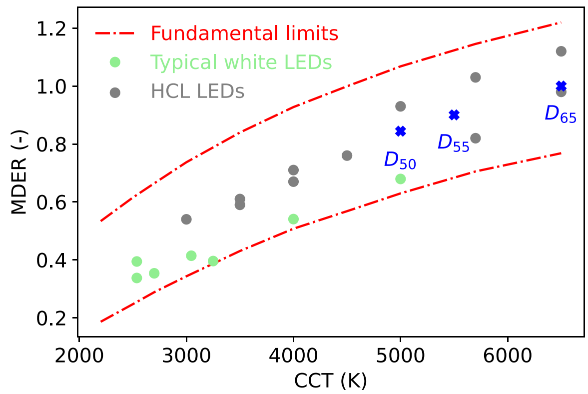

Fig. 2. Visualization of multiple typical white LEDs and the standard illuminants D_{50}, D_{55} and D_{65} within the fundamental spectral MDER boundaries ($R_f \geq 80$). It is clear that typical white LEDs offer fairly low MDER values. Some recent, commercialized HCL LEDs target higher MDER values, but there is still ample room for further improvement.

To close this gap, a previous study combined red-emissive CdSe/ZnS QDs, a yellow YaG:Ce phosphor and a blue 455nm-emitting LED chip to achieve a minimal MDER of 0.389 (2700K, CRI 95) and a maximal MDER of 1.223 (7808K, CRI 95) [33]. As mentioned before, cadmium is a restricted element, and the MDER values at lower CCT were still quite modest. In order to pursue higher spectral flexibility, multi-channel QD-LEDs with 4 to 6 channels have also been studied. By combining cadmium-free, perovskite QD-based LEDs in a multi-channel system with 6 channels, the MDER could be tuned in a range between 0.33 (2128K, R_f 87.3) and 1.104 (6459K, R_f 91.4) while altering the CCT [20]. Luminous efficacy values of up to 61.4 lm W^{-1} were obtained for the resulting six-channel system. A similar approach has been adopted in other research, with the focus slightly shifted to attaining higher luminous efficacy values [3,21].

3. Methods

3.1. Optical simulation model

For accurate predictions and optimization of the emitted spectral radiant flux by the quantum-dot-on-chip LED, an optical simulation model of the QD-LED package is considered that includes all relevant losses (e.g. package losses and re-absorption losses by the QDs). This optical simulation model is implemented in the commercial ray-tracing software LightTools, as described in earlier work [28,34]. For the LED package, a LUXEON 3535 LED from Lumileds is considered, consisting of a single blue LED chip with peak emission around 450 nm and a wall-plug efficiency of 70%. This LED package contains a transparent resin with a mixture of 3 different types of QDs on top of the blue LED chip. A picture of the simulated configuration and emission spectrum of the blue LED chip are shown in Fig. 3.

In order to achieve high MDER values, emission around 490 nm is crucial (see Fig. 1a). This requirement is achieved by considering InP-based cyan-emitting QDs with measured absorption and emission spectra as shown in Fig. 4a; cyan-emitting QDs have already been considered to replicate daylight spectra in the past [35,36]. For emission in the green-red spectral region, the model considers two different InP-based QDs with a variable emission peak location that depends directly on the QD core size. The impact of changing the InP-based QD core size (d_C) on the resulting QD emission and absorption is modeled according to an empirical QD model [37]. As can be seen in Fig. 4b, the InP-based QD core size determines both absorption and emission spectrum. Considering d_C as a variable in the optical model for two of the three QD types, allows for high spectral flexibility. For simplicity, the photoluminescence quantum yield (PLQY) of all QDs is initially set to 80%.

3.2. Parameter optimization

To optimize the emission spectrum of the QD-LED model, 5 parameters are varied: the concentrations of each QD type and the core size (d_C) of the two QDs for the red-green region. For each combination of these 5 parameters, the resulting output spectrum can be simulated using the model described in the previous section. This 5-parameter model is optimized using a global optimization algorithm, i.e. differential evolution (DE), which was introduced by Storn & Price in 1997 [38]. Optimizing the model parameters consists of forcing the output spectrum to satisfy the metric constraints in terms of D_{uv}, color rendering and the targeted CCT, while minimizing or maximizing the MDER. Sufficient perceived whiteness is obtained by limiting the D_{uv} tolerance to 0.006 according to ANSI C78.377.

3.3. QD-LED fabrication and characterization

For fabrication of the QD-LEDs, the LUXEON 3535 LED packages were filled with a slurry of three different InP-based QDs mixed within UV curable resin. Following the outcome of the optimization study, green-emitting QDs with peak emission at 528 nm (PLQY 85%), and red-emitting QDs with peak emission at 600 nm (PLQY 66%), shown in Fig. 5, were used in addition to the earlier mentioned cyan-emitting QDs emitting at 483 nm (PLQY 82%). The synthesis of all QDs followed a similar procedure as described in Tessier et al. (2015) and Van Avermaet et al. (2022) [26,39], and further details can be found in sections 1.1–1.3 of the supplementary material. After synthesis, the QDs were dispersed into a thiol-ene resin consisting of pentaerythritol tetrakis (3-mercaptopropionate) (PETMP), with a detailed explanation in section 1.4 of the supplementary material. To obtain the required

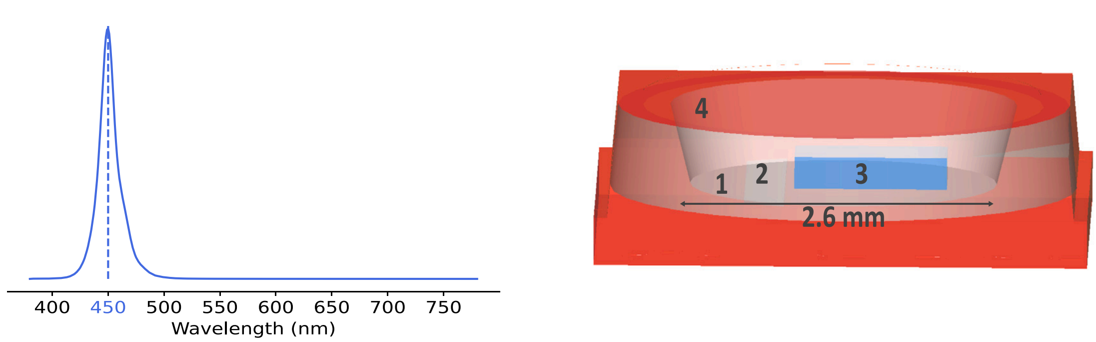

(a) (b)

Fig. 3. **(a)** Emission spectrum of the blue LED chip in the considered Lumileds LUXEON 3535 LED package. **(b)** 3D view of the simulated LED package with (1) bottom reflector, (2) diffusing bar, (3) blue LED chip, and (4) reflective cup which contains the QD mixture.

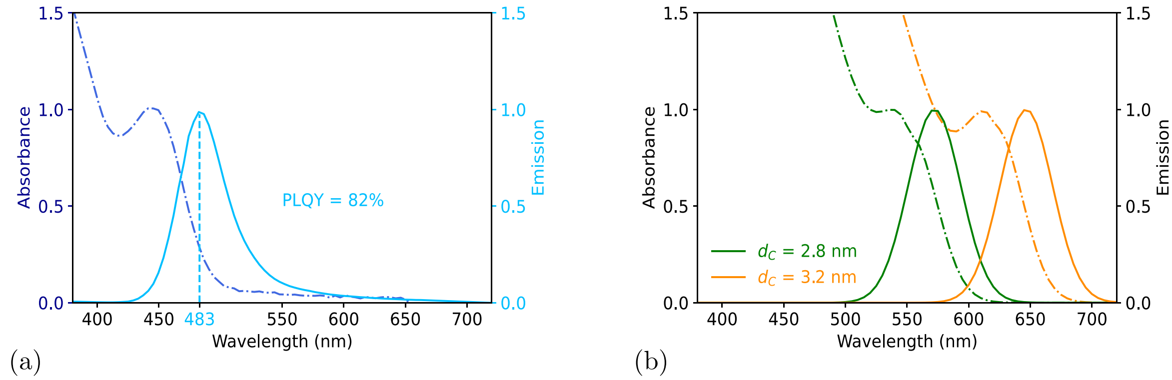

Fig. 4. **(a)** Measured emission and absorption spectrum of the InP-based cyan-emitting QD. **(b)** Impact of changing the core size for the used InP-based QD model; full lines represent the emission spectra, dashed lines show the absorbance. In **(a)** and **(b)**, the band-edge peak absorption and emission are normalized to 1.

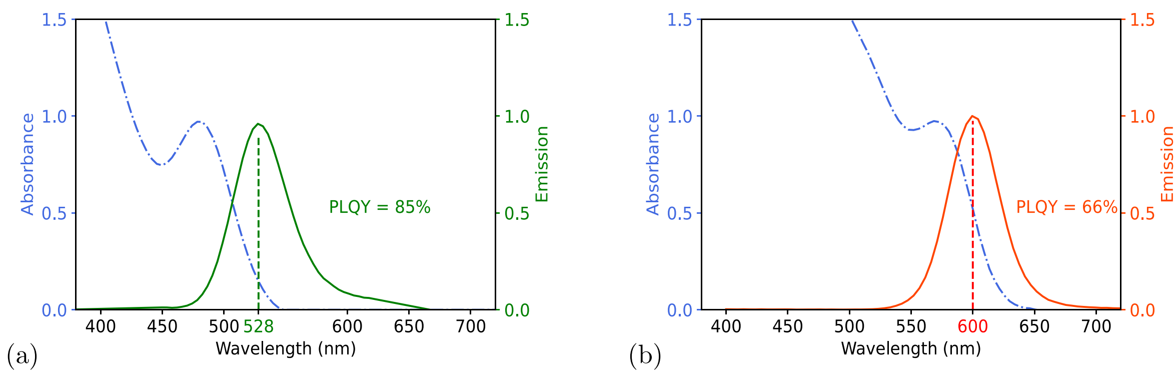

Fig. 5. The optical properties for the green **(a)** and red **(b)** QDs. These have PLQY of respectively 85% and 66%. The band-edge peak absorption and emission are normalized to 1.

concentrations of cyan, green and red-emitting QDs for reaching the targeted emission spectra, the separate QD-in-thiol-ene mixtures were mixed within a clear photopolymer resin from Formlabs, using the correct mass percentages [40]. The homogenized QD slurry was then deposited in the Luxeon LED recycling cavity with a micropipette, and cured with UV light with peak emission at 398 nm. To characterize the resulting spectral radiant flux of the emitted light, the LEDs were operated with a drive current of 10 mA and a typical forward voltage of 2.6 V. As mentioned earlier, the blue LEDs have an emission peak at 450 nm and wall-plug efficiency of 70% (±3.5%). The spectral radiant flux of the LEDs was measured with a custom-made integrating sphere [41].

4. Results

4.1. MDER optimization

The optical simulation model was optimized to reach minimal and maximal MDER at CCTs ranging from 2000K to 6500K, with an $R_f \geq 80$ constraint and a maximal D_{uv} deviation of 0.006. For each setting, the algorithm was terminated after 200 iterations without improvement (tolerance 5e−6). A detailed overview of the acquired MDER values is shown in Fig. 6, where these results are compared with the fundamental spectral boundaries under the same constraints. The acquired MDER values clearly indicate that a single-chip QD-LED with three types of QDs, including cyan-emitting QDs, can reach both very low and very high MDER values at all CCTs. For example, at 5000K, the QD model reaches a maximal MDER value that is at 90% of the fundamental spectral maximum and almost 40% above the D_{50} illuminant MDER. Looking at the shapes of the obtained spectra in Fig. 7, it is clear that all 3 QDs are essential for reaching the desired spectral performance. The cyan-emitting QDs play a crucial role in tailoring the MDER, by

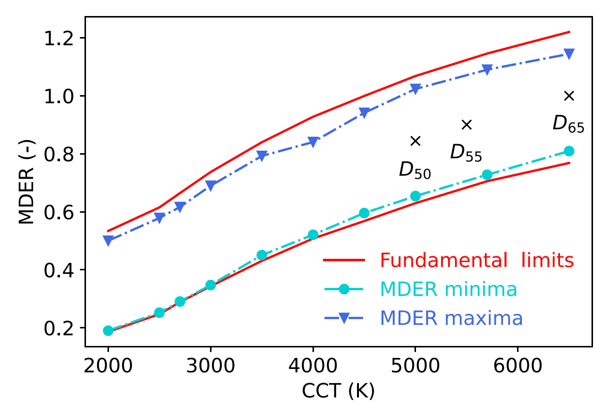

Fig. 6. The obtained minimal and maximal MDER values with the QD-LED simulation model for various CCTs, compared with the fundamental spectral MDER limits ($R_f \geq 80$ and $D_{uv} \leq 0.006$).

lowering or increasing their concentration respectively, while the other two QDs are needed for meeting the required color constraints.

4.2. Experimental QD-LEDs (1)

Using the obtained parameters from the optimization for the QD concentrations and core sizes, we tried to replicate the simulated QD-LED with maximal MDER at 5700K in practice. The measured spectral radiant flux for three different fabricated QD-LEDs is shown in Fig. 8a. One notices the very strong correlation between the obtained CCT and MDER. The measured spectral radiant flux with a CCT of 5571K is

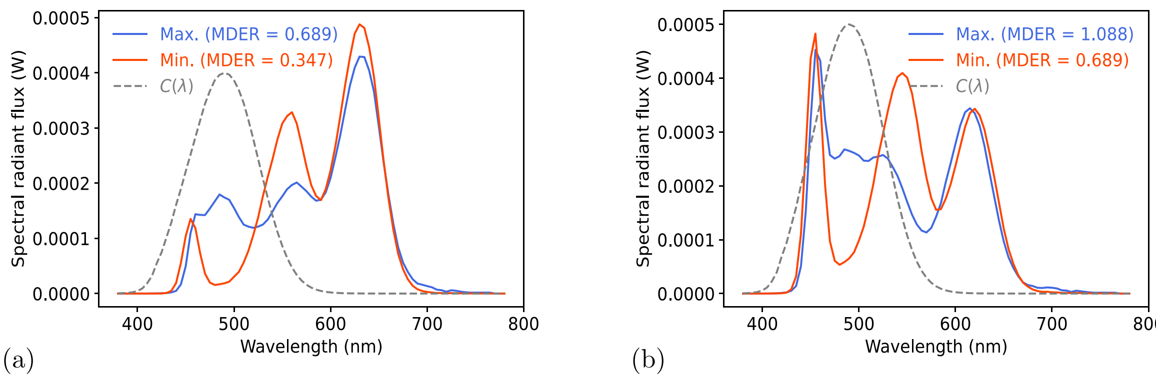

Fig. 7. MDER optimized spectra at **(a)** 3000K and **(b)** 5700K using the optical simulation model .

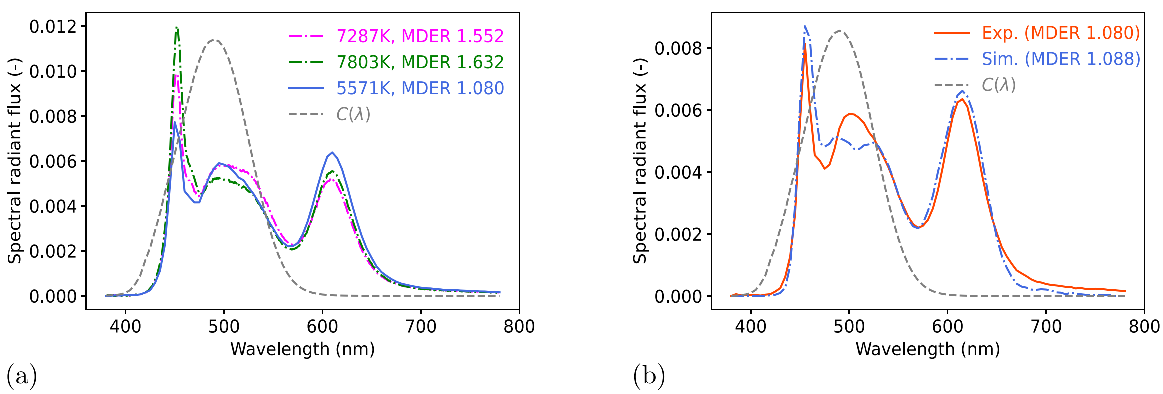

Fig. 8. (a) Measured normalized spectral radiant flux for three different fabricated QD-LEDs, targeting maximal MDER. **(b)** A comparison of the simulated (MDER = 1.088, CCT = 5700K) and experimental (MDER = 1.080, CCT = 5700K) spectra. The total radiant flux of the simulation result is re-scaled to the total radiant flux of the experimental result, to allow better assessment of the overall spectral shape.

compared in Fig. 8b with the simulated QD-LED spectrum with maximal MDER at 5700K. Although there is a good overall correspondence between the simulated and experimental spectrum, there is a clear deviation in the cyan region. This deviation is most likely caused by the strong self-absorption and re-absorption of the cyan-emitted light, by the cyan and green/red-emitting QDs, respectively. In principle, the optical simulations include these self- and re-absorption effects. However, small variations in the implemented absorption/emission spectrum compared to the real spectra, can give rise to significant deviations of the resulting output spectrum for wavelength regions with much self/re-absorption [42]. This effect is compounded by the fact that self-absorption makes it also very difficult to experimentally characterize the intrinsic QD absorption/emission spectra in their overlap region [43]. Despite this deviation in the important cyan region, the obtained MDER value of 1.080 is still very close to the simulated value of 1.088. To our knowledge, this experimentally obtained MDER value sets a new record for single-chip package white LEDs at this CCT.

In terms of other lighting parameters, the R_f of the simulated spectrum is 80.06, with a D_{uv} of 0.0009 and CIE 1976 LUV u'= 0.207, v'= 0.476. For luminous efficacy, the simulated LED reaches 97 lm W^{-1}, while the experimental QD-LED reaches an efficacy of 62 lm W^{-1}. These relatively low values can again be attributed to the multiple self- and re-absorption effects that occur, especially in the crucial cyan/green area. These self- and re-absorption effects are known for having a detrimental effect on the overall efficiency of QD-LEDs, when using QDs with a non-unity PLQY [28]. These QD-LED losses are also combined with a circadian target metric that only considers the circadian/luminous flux ratio. This important aspect of circadian optimized light sources is further discussed in the next section.

5. Discussion

5.1. Balancing melanopic and luminous efficacy

When considering the spectral shape of $C(\lambda)$ and $V(\lambda)$ in Fig. 1, it is clear that there is an inherent trade-off between melanopic radiant flux and luminous flux when optimizing the SPD of a light source, as already indicated in past research [32]. Furthermore, when considering equation (2), it is important to note that the MELR and MDER actually scale the melanopic radiant flux with the luminous flux. This implies that it is actually possible to obtain higher MDER values by reducing both melanopic and luminous flux, as long as the latter decreases more than the first. Optimizing SPDs for high MDER can thus lead to inefficient systems, both in terms of luminous efficacy and circadian efficacy; an aspect that is seldom considered in previous research.

To analyze this delicate balance, a spectral optimization was performed following the methodology of Cerpentier and Meuret (2021), that maximizes the melanopic radiant flux of a flexible parametrized SPD with 1 W of optical power, when constraining MDER to different values in the range of minimal and maximal MDER at 5700K and $R_f \geq 80$ [32]. When dividing the obtained melanopic radiant flux and corresponding luminous flux by the considered optical power, one obtains circadian efficacy of radiation (CER) and luminous efficacy of radiation (LER); the former is expressed in biolumen (blm) per Watt, a circadian equivalent of lumen [3]. The obtained results for each MDER value are visualized in Fig. 9. This figure first of all confirms that spectra with maximal MDER values are indeed acquired by reducing both melanopic and luminous radiant flux. Such spectra are therefore only useful in situations where maximal circadian impact is desired for

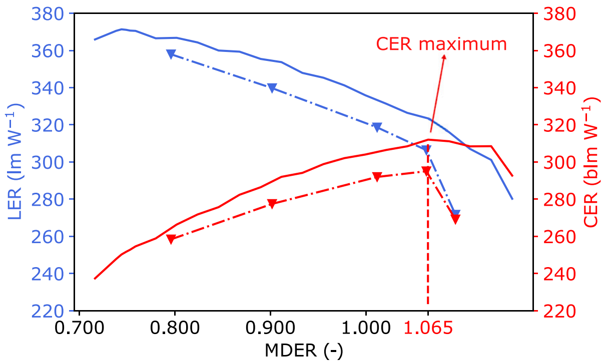

Fig. 9. Maximal circadian efficacy of radiation (CER, blm W^{-1}) and luminous efficacy of radiation (LER, lm W^{-1}) for various MDER targets, when optimizing the melanopic radiant flux of a flexible parametrized spectrum (full lines), and the optical QD-LED model (dashed lines). The trend is similar for both parametric models.

a fixed luminous output, and energy consumption is of no concern. In most cases however, consumed energy is important, and Fig. 9 shows that spectra with less extreme MDER actually provide both higher CER and LER. Taking this insight into account, the QD-LED optical model was also re-optimized to obtain maximal melanopic radiant flux for various MDER values (5700K, $R_f \geq 80$). The resulting CER and LER values with this QD-LED optical model also are added to Fig. 9, and these confirm that significantly higher LER and CER can be obtained for slightly lower MDER.

5.2. Experimental QD-LEDs (2)

To realize a QD-LED with higher luminous (and circadian) efficacy compared to the QD-LED described in Section 4.2, several adjustments to the QD-LED package configuration, used materials and target spectrum were made. First of all, the simulated QD-LED spectrum that was optimized for maximal melanopic radiant flux, instead of maximal MDER, was used as spectral target. This allows improving both the luminous efficacy and circadian efficacy of the considered QD-LEDs, as explained in previous section. Second, new batches of red and green-emitting QDs were synthesized with emission spectra in correspondence with this new QD-LED target spectrum. The experimental peak emission wavelength of the green-emitting QDs was changed from 528 to 511 nm, while the peak emission of the red-emitting QDs was changed from 600 to 585 nm. The PLQY of the new red-emitting QDs was improved from 66% to 78%, while the PLQY of the green-emitting QDs remained at around 85%,with a detailed description of the synthesis in section 1.3 of the supplementary material. Aside from the individual QD efficiencies, the QD LED configuration itself can be optimized to reduce re-absorption effects. Past research has shown the potential of stacking layers of QDs in a specific order to reduce these re-absorption effects [44–46]. Other approaches highlight the possibility of placing the QDs at a distance with respect to the LED chip, in a "remote phosphor" configuration [47,48]. An approach with much potential for on-chip QD LEDs is adding (part of) the QDs in a hemispherical dome on top of the blue LED (package) to improve the light extraction efficiency [28,29]. We employ a similar approach to enhance the efficiency of the QD-LED, by putting only the green and red-emitting QDs in the blue LED package, and incorporating the cyan-emitting QDs in such a dome-like structure . This configuration improves the extraction efficiency, while integrating also the idea of stacking QD layers to reduce re-absorption losses (Fig. 10a). This approach was demonstrated to improve the luminous efficacy of RGB QD-LEDs in previous work [28].

The combination of separating the cyan-emitting QDs in a dome, using red-emitting QDs with higher PLQY and targeting a spectral shape with higher CER and LER, led to an increase of 30% in luminous efficacy, to 80 lm W^{-1}. Aside from this significant increase in luminous efficacy, also the circadian luminous efficacy (CLE) – the amount of bi-olumen per consumed electrical power – rose with 24% in comparison to the first experimental QD-LED; this results in a CLE of 74 blm W^{-1}. The LER and CER respectively reach high values of 312 lm W^{-1} and 292 blm W^{-1}, reflecting the optimized spectral shape that follows from the CER-targeted optimization. The measured spectrum has a CCT of 5501 and D_{uv} of 0.0014 (u'= 0.206, v'= 0.479), which classifies it as a white QD-LED.

5.3. Overview

Table 1 shows the measured specifications for the two experimental QD-LEDs with CCT ≈ 5500K that are described in this paper. These results are compared with commercially available white LEDs (including circadian optimized LEDs) and past literature on single- and multi-channel QD-LEDs that target maximal circadian effects. Despite differences in CCT and color rendering, the following important conclusions can be drawn: although a single LED chip is used, the spectral flexibility achieved by mixing 3 QD types (including cyan-emitting QDs) allows for state-of-the-art MDER and CER values, even when comparing to multi-channel solutions. The obtained LER values are also highly competitive. In order to consider the electrical and optical power losses in the LED chip and package, the LE and CLE values are also reported in Table 1. These measured values of the demonstrated single-chip QD-LEDs are more moderate, especially when comparing with recent commercial circadian-optimized LEDs. Aside from the slight reduction in energy efficiency due to our higher MDER values (Fig. 9), the deficiency can largely be attributed to limited fabrication resources.

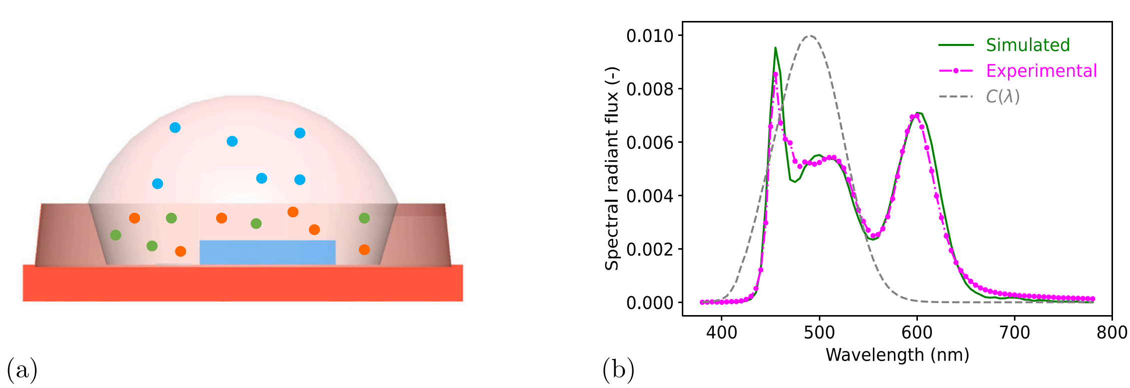

Fig. 10. **(a)** The QD-LED configuration with a dome-like structure filled with cyan-emitting QDs. The reflecting cavity contains a mixture of green and red-emitting QDs. **(b)** A comparison of the simulated and experimental normalized spectra that follow from the CER-based optimization. The final experimental spectrum has a luminous efficacy of 80 lm W^{-1} with an MDER value of 1.031.

Table 1
Comparison of figures of merit for the D_{65} illuminant, various commercially available LEDs and past research on single- and multi-channel QD-based circadian light sources. The table highlights how the investigated single-chip QD-LEDs in this paper set a new standard in terms of spectral circadian performance, as is reflected by the obtained MDER and CER values.

		CCT (K)	MDER (–)	CER (blm W^{-1})	CLE (blm W^{-1})	LER (lm W^{-1})	LE (lm W^{-1})	R_f (*) R_a (**)
D_{65} illuminant		6500	1	186	–	206	–	100*
Typical white LED 1[a]		5060	0.68	203	31	329	50	77*
Typical white LED 2[b]		3030	0.41	114	21	305	56	82*
HCL LED 1[c]		5700	0.82	236	117	319	157	80**
HCL LED 2[d]		5700	1.03	270	126	290	135	80**
4-channel WLED	[3]	6584	1.02	258	88	280	96	94**
5-channel WLED	[20]	5132	0.88	217	45	260	56	82*
6-channel WLED 1	[20]	4952	0.88	218	32	289	55	91*
6-channel WLED 2	[21]	5500	0.95	276	–	321	–	93**
Single-chip, Cd QD-LED	[33]	5388	0.84	–	88	–	116	96**
Experimental QD-LED 1		5571	**1.08**	284	61	291	62	80*
Experimental QD-LED 2		5501	1.03	**293**	74	312	80	78*

[a]The Globe A19 domestic LED.
[b]The Sylvania G25 domestic LED.
[c]The OSCONIQ E2835 Cyan.
[d]The samsung LM302N Day.

The used blue LED chips have an external quantum efficiency of 70%, while recent state-of-the-art blue LED chips have reached efficiencies over 80% [49]. Additionally, the used InP-based QDs in this study have PLQY's of 85% or lower, while it has been shown that quantum efficiencies of over 90% can be achieved [50,51]. If we consider these state-of-the-art values (EQE LED ≥ 80%, PLQY QD ≥ 90%) in the optical simulation model, LE and CLE values of over 140 (b)lm W^{-1} can be reached with the current single-chip QD-LED configuration.

6. Conclusions

Spectral engineering of solid-state light sources has resulted in high luminous efficiency combined with optimal color rendering. There is however a clear trend in the lighting industry to also consider the non-visual effects of light, quantified e.g. by the melanopic daylight efficacy ratio (MDER) or circadian luminous efficacy of radiation(CER). While significant progress has already been made over a short amount of time, the spectral shapes of these circadian-targeted systems still leave ample room for improvement. In this paper, a method to optimize the spectral circadian performance of single-chip QD LEDs, including cyan-emitting QDs, was introduced. Following the results of this procedure, we fabricated a QD-LED that realizes a new MDER record at its corresponding CCT of 5570K. While a light source with maximal MDER can be useful in settings where energy consumption is of no concern, a discussion on the importance of considering both CER and MDER when designing efficient human-centric-lighting LEDs was added. Following this discussion, a second QD-LED was demonstrated that reaches record-breaking CER at 5500K while maintaining a high MDER value.

CRediT authorship contribution statement

Jeroen Cerpentier: Conceptualization, Methodology, Software, Validation, Formal analysis, Investigation, Writing – original draft, Writing – review & editing, Visualization. **Bega Karadza:** Methodology, Validation, Formal analysis, Investigation, Writing – original draft. **Hannes van Avermaet:** Resources, Methodology, Writing – review & editing, Investigation, Validation. **Luca Giordano:** Resources, Methodology, Writing – review & editing, Investigation, Validation. **Pieter Schiettecatte:** Resources, Methodology, Writing – review & editing, Investigation, Validation. **Zeger Hens:** Conceptualization, Writing – review & editing, Supervision, Project administration, Funding acquisition. **Youri Meuret:** Conceptualization, Methodology, Validation, Investigation, Writing – original draft, Writing – review & editing, Supervision, Project administration, Funding acquisition.

Declaration of competing interest

The authors declare that they have no known competing financial interests or personal relationships that could have appeared to influence the work reported in this paper.

Data availability

Data will be made available on request.

Acknowledgments

We are grateful to Lumileds for providing us with a large batch of empty 3535 LED packages and relevant information about this specific package.

Funding

This work was supported by SIM-Flanders [grant numbers SBO-QDOCCO, SBO-QUALIDI]; Z.H. also acknowledges research funding from Ghent University [grant number BOF-GOA G01019]; P.S. acknowledges the FWO-Vlaanderen [grant number 1S40117N] and VLAIO [AIO.ONO.2020.0007.01].

Appendix A. Supplementary data

Supplementary material related to this article can be found online at https://doi.org/10.1016/j.optlastec.2023.109839.

References

[1] W. Zhao, B. Xie, Y. Peng, S. Xue, X. Luo, R. Hu, Cooling photoluminescent phosphors in laser-excited white lighting with three-dimensional boron nitride networks, Opt. Laser Technol. 157 (2023) 108689, http://dx.doi.org/10.1016/j.optlastec.2022.108689.

[2] H. Liu, Y. Fu, B.Z. Tang, Z. Zhao, All-fluorescence white organic light-emitting diodes with record-beating power efficiencies over 130 lm W–1 and small roll-offs, Nature Commun. 13 (1) (2022) 5154, http://dx.doi.org/10.1038/s41467-022-32967-w.

[3] J. Hye Oh, S. Ji Yang, Y. Rag Do, Healthy, natural, efficient and tunable lighting: four-package white LEDs for optimizing the circadian effect, color quality and vision performance, Light Sci. Appl. 3 (2) (2014) e141, http://dx.doi.org/10.1038/lsa.2014.22.

[4] N. Sandor, H. Yaguchi, CIE expert symposium on LED light sources: Physical measurement and visual and photobiological assessment, Color Res. Appl. 29 (2) (2004) 168, http://dx.doi.org/10.1002/col.10242.

[5] M.P. Royer, Tutorial: Background and guidance for using the ANSI/IES TM-30 method for evaluating light source color rendition, Leukos 18 (2) (2022) 191–231, http://dx.doi.org/10.1080/15502724.2020.1860771.
[6] B. Mitchell, R. Wei, J. Takatsu, D. Timmerman, T. Gregorkiewicz, W. Zhu, S. Ichikawa, J. Tatebayashi, Y. Fujiwara, V. Dierolf, Color-tunablility in GaN LEDs based on atomic emission manipulation under current injection, ACS Photonics 6 (5) (2019) 1153–1161, http://dx.doi.org/10.1021/acsphotonics.8b01461.
[7] J. Nie, Z. Chen, F. Jiao, J. Zhan, Y. Chen, Y. Chen, Z. Pan, X. Kang, Y. Wang, Q. Wang, et al., Low blue light hazard for tunable white light emitting diode with high color fidelity and circadian performances, Opt. Laser Technol. 135 (2021) 106709, http://dx.doi.org/10.1016/j.optlastec.2020.106709.
[8] K. Thapan, J. Arendt, D.J. Skene, An action spectrum for melatonin suppression: evidence for a novel non-rod, non-cone photoreceptor system in humans, J. Physiol. 535 (1) (2001) 261–267, http://dx.doi.org/10.1111/j.1469-7793.2001.t01-1-00261.x.
[9] J. Nie, Z. Chen, F. Jiao, J. Zhan, Y. Chen, Z. Pan, C. Deng, X. Xi, X. Kang, Y. Wang, et al., Optimization of the dynamic light source considering human age effect on visual and non-visual performances, Opt. Laser Technol. 145 (2022) 107463, http://dx.doi.org/10.1016/j.optlastec.2021.107463.
[10] M. Spitschan, Melanopsin contributions to non-visual and visual function, Curr. Opin. Behav. Sci. 30 (2019) 67–72, http://dx.doi.org/10.1016/j.cobeha.2019.06.004.
[11] K. Houser, P. Boyce, J. Zeitzer, M. Herf, Human-centric lighting: Myth, magic or metaphor? Light. Res. Technol. (2020) 1477153520958448, http://dx.doi.org/10.1177/1477153520958448.
[12] S. Ye, F. Xiao, Y. Pan, Y. Ma, Q. Zhang, Phosphors in phosphor-converted white light-emitting diodes: Recent advances in materials, techniques and properties, Mater. Sci. Eng. R 71 (1) (2010) 1–34, http://dx.doi.org/10.1016/j.mser.2010.07.001.
[13] Q. Dai, Q. Shan, H. Lam, L. Hao, Y. Lin, Z. Cui, Circadian-effect engineering of solid-state lighting spectra for beneficial and tunable lighting, Opt. Express 24 (18) (2016) 20049–20059, http://dx.doi.org/10.1364/OE.24.020049.
[14] Y. Mei, G.-E. Weng, B.-P. Zhang, J.-P. Liu, W. Hofmann, L.-Y. Ying, J.-Y. Zhang, Z.-C. Li, H. Yang, H.-C. Kuo, Quantum dot vertical-cavity surface-emitting lasers covering the 'green gap', Light Sci. Appl. 6 (1) (2017) e16199, http://dx.doi.org/10.1038/lsa.2016.199.
[15] B. Karadza, H. Van Avermaet, L. Mingabudinova, Z. Hens, Y. Meuret, Efficient, high-CRI white LEDs by combining traditional phosphors with cadmium-free InP/ZnSe red quantum dots, Photonics Res. 10 (1) (2022) 155–165, http://dx.doi.org/10.1364/PRJ.428843.
[16] S. Sadeghi, B.G. Kumar, R. Melikov, M.M. Aria, H.B. Jalali, S. Nizamoglu, Quantum dot white LEDs with high luminous efficiency, Optica 5 (7) (2018) 793–802, http://dx.doi.org/10.1364/OPTICA.5.000793.
[17] A. Onal, G.O. Eren, S. Sadeghi, R. Melikov, M. Han, O. Karatum, M.S. Ozer, H. Bahmani Jalali, I.B. Dogru-Yuksel, I. Yilgor, et al., High-performance white light-emitting diodes over 150 lm/W using near-unity-emitting quantum dots in a liquid matrix, ACS Photonics 9 (4) (2022) 1304–1314, http://dx.doi.org/10.1021/acsphotonics.1c01805.
[18] J.S. Steckel, J. Ho, S. Coe-Sullivan, et al., QDs generate light for next-generation displays, Photonics Spectra 48 (9) (2014) 55–61.
[19] Y. Shirasaki, G.J. Supran, M.G. Bawendi, V. Bulović, Emergence of colloidal quantum-dot light-emitting technologies, Nat. Photonics 7 (1) (2013) 13–23, http://dx.doi.org/10.1038/nphoton.2012.328.
[20] H.C. Yoon, J.H. Oh, S. Lee, J.B. Park, Y.R. Do, Circadian-tunable perovskite quantum dot-based down-converted multi-package white LED with a color fidelity index over 90, Sci. Rep. 7 (1) (2017) 1–11, http://dx.doi.org/10.1038/s41598-017-03063-7.
[21] Z. He, C. Zhang, H. Chen, Y. Dong, S.-T. Wu, Perovskite downconverters for efficient, excellent color-rendering, and circadian solid-state lighting, Nanomaterials 9 (2) (2019) 176, http://dx.doi.org/10.3390/nano9020176.
[22] Z. Qin, K. Wang, F. Chen, X. Luo, S. Liu, Analysis of condition for uniform lighting generated by array of light emitting diodes with large view angle, Opt. Express 18 (16) (2010) 17460–17476, http://dx.doi.org/10.1364/OE.18.017460.
[23] S.K. Abeysekera, V. Kalavally, M. Ooi, Y.C. Kuang, Impact of circadian tuning on the illuminance and color uniformity of a multichannel luminaire with spatially optimized LED placement, Opt. Express 28 (1) (2020) 130–145, http://dx.doi.org/10.1364/OE.381115.
[24] P. Yu, S. Cao, Y. Shan, Y. Bi, Y. Hu, R. Zeng, B. Zou, Y. Wang, J. Zhao, Highly efficient green inp-based quantum dot light-emitting diodes regulated by inner alloyed shell component, Light Sci. Appl. 11 (1) (2022) 162, http://dx.doi.org/10.1038/s41377-022-00855-z.
[25] B. Chen, D. Li, F. Wang, InP quantum dots: synthesis and lighting applications, Small 16 (32) (2020) 2002454, http://dx.doi.org/10.1002/smll.202002454.
[26] H. Van Avermaet, P. Schiettecatte, S. Hinz, L. Giordano, F. Ferrari, C. Nayral, F. Delpech, J. Maultzsch, H. Lange, Z. Hens, Full-spectrum InP-based quantum dots with near-unity photoluminescence quantum efficiency, ACS Nano 16 (6) (2022) 9701–9712, http://dx.doi.org/10.1021/acsnano.2c03138.
[27] Q. Li, J. Bai, M. Huang, L. Li, X. Liao, L. Wang, B. Xu, X. Jin, High-performance, environmentally friendly solid-phase color converted-based quantum dots white light-emitting diodes, J. Lumin. 255 (2023) 119560, http://dx.doi.org/10.1016/j.jlumin.2022.119560.
[28] B. Karadza, H. Van Avermaet, L. Mingabudinova, Z. Hens, Y. Meuret, Comparison of different RGB InP-quantum-dot-on-chip LED configurations, Opt. Express 30 (24) (2022) 43522–43533, http://dx.doi.org/10.1364/OE.476135.
[29] J.-S. Li, Y. Tang, Z.-T. Li, J.-X. Li, X.-R. Ding, B.-H. Yu, S.-D. Yu, J.-Z. Ou, H.-C. Kuo, Toward 200 lumens per watt of quantum-dot white-light-emitting diodes by reducing reabsorption loss, ACS Nano 15 (1) (2020) 550–562, http://dx.doi.org/10.1021/acsnano.0c05735.
[30] L.J. Schlangen, L.L. Price, The lighting environment, its metrology, and non-visual responses, Front. Neurol. 12 (2021) 624861, http://dx.doi.org/10.3389/fneur.2021.624861.
[31] CIE System for Metrology of Optical Radiation for iPRGC-Influenced Responses to Light, CIE Vienna, Austria, 2018, p. 32.
[32] J. Cerpentier, Y. Meuret, Fundamental spectral boundaries of circadian tunability, IEEE Photonics J. 13 (4) (2021) 1–5, http://dx.doi.org/10.1109/JPHOT.2021.3098903.
[33] B. Xie, J. Zhang, W. Chen, J. Hao, Y. Cheng, R. Hu, D. Wu, K. Wang, X. Luo, Realization of wide circadian variability by quantum dots-luminescent mesoporous silica-based white light-emitting diodes, Nanotechnology 28 (42) (2017) 425204, http://dx.doi.org/10.1088/1361-6528/aa82d7.
[34] LightTools 8.7.0, Synopsys Optical Solutions, Mountain view, California, 2019.
[35] C. Samarakoon, H.W. Choi, S. Lee, X.-B. Fan, D.-W. Shin, S.Y. Bang, J.-W. Jo, L. Ni, J. Yang, Y. Kim, et al., Optoelectronic system and device integration for quantum-dot light-emitting diode white lighting with computational design framework, Nature Commun. 13 (1) (2022) 4189, http://dx.doi.org/10.1038/s41467-022-31853-9.
[36] A. Hong, J. Kim, J. Kwak, Sunlike white quantum dot light-emitting diodes with high color rendition quality, Adv.Opt. Mater. 8 (22) (2020) 2001051, http://dx.doi.org/10.1002/adom.202001051.
[37] J. Ryckaert, A. Correia, M.D. Tessier, D. Dupont, Z. Hens, P. Hanselaer, Y. Meuret, Selecting the optimal synthesis parameters of InP/CdxZn 1- x Se quantum dots for a hybrid remote phosphor white LED for general lighting applications, Opt. Express 25 (24) (2017) A1009–A1022, http://dx.doi.org/10.1364/OE.25.0A1009.
[38] R. Storn, K. Price, Differential evolution–a simple and efficient heuristic for global optimization over continuous spaces, J. Global Optim. 11 (4) (1997) 341–359, http://dx.doi.org/10.1023/A:1008202821328.
[39] M.D. Tessier, D. Dupont, K. De Nolf, J. De Roo, Z. Hens, Economic and size-tunable synthesis of InP/ZnE (E=S, Se) colloidal quantum dots, Chem. Mater. 27 (13) (2015) 4893–4898, http://dx.doi.org/10.1021/acs.chemmater.5b02138.
[40] Clear Resin, Formlabs Inc., Somerville, Massachusetts, United States.
[41] P. Hanselaer, A. Keppens, S. Forment, W.R. Ryckaert, G. Deconinck, A new integrating sphere design for spectral radiant flux determination of light-emitting diodes, Meas. Sci. Technol. 20 (9) (2009) http://dx.doi.org/10.1088/0957-0233/20/9/095111.
[42] W. Zhang, D. Dai, X. Chen, X. Guo, J. Fan, Red shift in the photoluminescence of colloidal carbon quantum dots induced by photon reabsorption, Appl. Phys. Lett. 104 (9) (2014) 091902, http://dx.doi.org/10.1063/1.4867487.
[43] G. Gu, Z. Zheng, H. Zhang, Y. Zhang, Z. Gan, R. Huang, X. Zhang, Re-absorption-free perovskite quantum dots for boosting the efficiency of luminescent solar concentrator, J. Lumin. 248 (2022) 118963, http://dx.doi.org/10.1016/j.jlumin.2022.118963.
[44] D. Cai, X. Yuan, D. Zhu, H. Zhou, H. Li, J. Zhao, Phosphor geometry regulations with separated red and green quantum dot layers for high performance warm white light-emitting diodes, Mater. Res. Bull. 85 (2017) 222–227, http://dx.doi.org/10.1016/j.materresbull.2016.09.026.
[45] Y. Tang, H. Lu, J. Li, Z. Li, X. Du, X. Ding, B. Yu, Improvement of optical and thermal properties for quantum dots WLEDs by controlling layer location, IEEE Access 7 (2019) 77642–77648, http://dx.doi.org/10.1109/ACCESS.2019.2919729.
[46] X. Peng, Low-cost and high-color-quality white light emitting diodes based on CdSe/ZnS quantum dots, J. Opt. 44 (2015) 249–254, http://dx.doi.org/10.1007/s12596-015-0253-x.
[47] X. Lei, H. Zheng, X. Guo, J. Chu, S. Liu, P. Liu, Optical performance enhancement of quantum dot-based light-emitting diodes through an optimized remote structure, IEEE Trans. Electron Devices 63 (2) (2015) 691–697, http://dx.doi.org/10.1109/TED.2015.2508026.
[48] M.-H. Shin, H.-G. Hong, H.-J. Kim, Y.-J. Kim, Enhancement of optical extraction efficiency in white LED package with quantum dot phosphors and air-gap structure, Appl. Phys. Express 7 (5) (2014) 052101, http://dx.doi.org/10.7567/APEX.7.052101.
[49] J. Piprek, Energy efficiency analysis of gan-based blue light emitters, ECS J. Solid State Sci. Technol. 9 (1) (2019) 015008, http://dx.doi.org/10.1149/2.0262001JSS.
[50] Y.-H. Won, O. Cho, T. Kim, D.-Y. Chung, T. Kim, H. Chung, H. Jang, J. Lee, D. Kim, E. Jang, Highly efficient and stable InP/ZnSe/ZnS quantum dot light-emitting diodes, Nature 575 (7784) (2019) 634–638, http://dx.doi.org/10.1038/s41586-019-1771-5.
[51] H.S. Shim, M. Ko, S. Nam, J.H. Oh, S. Jeong, Y. Yang, S.M. Park, Y.R. Do, J.K. Song, InP/ZnSeS/ZnS quantum dots with high quantum yield and color purity for display devices, ACS Appl. Nano Mater. (2023) http://dx.doi.org/10.1021/acsanm.2c04936.